Invited Paper

Sensor Fusion and Damage Classification in Composite Materials

Wenfan Zhou*[a], Whitney D. Reynolds[b], Albert Moncada[b], Narayan Kovvali[a], Aditi Chattopadhyay[b], Antonia Papandreou-Suppappola[a], and Douglas Cochran[a]

[a]Department of Electrical Engineering, Arizona State University, Tempe, AZ
[b]Department of Mechanical and Aerospace Engineering, Arizona State University, Tempe, AZ

ABSTRACT

We describe a statistical method for the classification of damage in complex structures. Our approach is based on a Bayesian framework using hidden Markov models (HMMs) to model time-frequency features extracted from structural data. We also propose two different methods for sensor fusion to combine information from multiple distributed sensors such that the overall classification performance is increased. The proposed approaches are applied to the classification and localization of delamination in a laminated composite plate. Results using both discrete and continuous observation density HMMs, together with the sensor fusion, are presented and discussed.

Keywords: structural health monitoring, damage detection and classification, hidden Markov models, sensor fusion

1. INTRODUCTION

There is currently a lot of research interest in the area of structural health monitoring (SHM)[1,2] in civil and aerospace engineering. A successful SHM system necessitates integration of solutions to multiple tasks from different areas. Among all these tasks, the development of effective damage detection and classification schemes is one major component of the SHM framework. In recent years, various signal processing techniques have been developed for damage identification, such as those based on wavelet transforms,[3–6] the matching pursuit decomposition,[7–9] and autoregressive models.[10,11] Although these deterministic methodologies have been applied to provide discriminatory damage features in many SHM problems, they do not rigorously explore uncertainty that is inherent in the structural characterization. In this context, statistical methods are needed to determine the damage state of a structure by modeling the statistical distribution of the derived features from that structure. Some statistical methods introduced for damage monitoring include Bayesian probabilistic inference methods,[12,13] artificial neural networks (ANN),[14] outlier analysis,[15–17] and support vector machines (SVM).[18] The general consensus is that successful structural damage characterization scheme is more likely to result from the combination of deterministic and statistical methods.

In this paper, a damage classification technique based on the use of the hidden Markov model (HMM)[19,20] first proposed by the authors in[21,22] is applied to classify damage in a composite structure. Time-frequency-scale features are first extracted from structural data using the matching pursuit decomposition (MPD)[23] algorithm. These are then modeled with Markov random processes using the HMM, and classification is then performed efficiently in a Bayesian framework. By capturing the statistical properties characterizing the underlying wave propagation, the HMM naturally leads to a more reliable and effective condition monitoring system. In the current paper both discrete and continuous HMMs are utilized. By modeling the continuous damage features directly, the continuous HMM tends to yield more accurate classification results. Experimentally collected data is used to construct and verify the HMMs. In addition, we describe two different sensor fusion procedures. The capability of the proposed classifier is demonstrated by application to the classification of delamination damage in a laminated composite.

The remainder of this paper is organized as follows. Section 2 reviews the basic algorithms used by the classifier. Section 3 discusses two different approaches of the sensor fusion process. Section 4 presents the

*wenfan.zhou@asu.edu; phone 1 480 965 5954

Modeling, Signal Processing, and Control for Smart Structures 2008, edited by Douglas K. Lindner
Proc. of SPIE Vol. 6926, 69260N, (2008) · 0277-786X/08/$18 · doi: 10.1117/12.776608

classifier performance (with and without sensor fusion) by application to delamination damage classification on a laminated composite.

2. HIDDEN MARKOV MODEL BASED DAMAGE CLASSIFIER

2.1 Matching Pursuit Decomposition based Feature Extraction

The critical first step for successful damage classification is the effective extraction of discriminatory features between different damage signals. Feature extraction also achieves a compact representation of available measured data. In this paper, we employed a feature extraction method based on the matching pursuit decomposition (MPD).[23] The MPD represents a signal $s(t)$ by a linear combination of basis functions (atoms) chosen from a redundant dictionary as

$$s(t) = \sum_{l=0}^{L-1} \alpha_l \, g_{\gamma l}(t) + R_L s(t), \tag{1}$$

where $\alpha_l = \int_{-\infty}^{\infty} R_l s(t) g^*_{\gamma l}(t) dt$ $(l = 1, \ldots, L)$ is the inner-product of the atom $g_{\gamma l}(t)$ with the residual signal $R_l s(t)$. The MPD iteratively selects atoms from the dictionary which yield the maximum projection $|\alpha_l|$ on to the residue $R_l s(t)$. The larger the number L of atoms selected and used, the more accurate is the representation (and the smaller the residue).

The dictionary used here is composed of the time-frequency shifted and scaled Gaussian atoms,

$$g_{\gamma l}(t) = e^{-\kappa_l^2 (t-\tau_l)^2} \cos(2\pi\nu_l t). \tag{2}$$

Where κ is the scaling factor, τ is the time shift and ν is the frequency shift. With these basis functions, the MPD extracts dominant signal components localized at different times, frequencies and scales. Each term in the MPD expansion in (1) can be fully characterized by the four parameters $\{\alpha, \kappa, \tau, \nu\}$. These four parameters then become a four-dimensional (4-D) feature vector $O = \{\alpha, \kappa, \tau, \nu\}$. Thus a signal with L MPD iterations can be represented by a sequence of feature vectors $\mathbf{O} = \{O_0, \ldots, O_{L-1}\}$, with $O_l = \{\alpha_l, \kappa_l, \tau_l, \nu_l\}$. The extracted sequence of feature vectors forms a length-L observation sequence to be modeled by a hidden Markov model (HMM).[20]

2.2 Hidden Markov Modeling and Classification

The hidden Markov model (HMM) is a stochastic method to model sequential data. The HMM defines underlying (non-observable or hidden) regions of stationarity known as states and models the inter-state transitions and in-state observation statistics with a Markov random process. Specifically, to model an observation sequence $\mathbf{O} = \{O_0, \ldots, O_{L-1}\}$ of length L, a HMM introduces N distinct underlying states $\mathbf{S} = \{S_1, S_2, ..., S_N\}$ with each O being in one of these N states. Let $Q = \{q_0, q_2, \ldots, q_{L-1}\}$ denotes the corresponding state sequence of $\mathbf{O}$. Assumming statistical independence of the observances O, the probability of $\mathbf{O}$, given the HMM λ, $P(\mathbf{O}|\lambda)$ can be expressed as

$$P(\mathbf{O}|\lambda) = \sum_{\text{all } Q} P(\mathbf{O}, Q|\lambda) = \sum_{\text{all } Q} \pi_{q_0} \cdot b_{q_0}(O_0) \cdot a_{q_0 q_1} \cdot b_{q_1}(O_1) \cdots a_{q_{L-2} q_{L-1}} \cdot b_{q_{L-1}}(O_{L-1}). \tag{3}$$

where π_{q_0} denotes the probability of the initial state to be q_0, $a_{q_l q_{l+1}}$ the transition probability from state q_l to state q_{l+1}, $b_{q_l}(O_l)$ the probability of observance to be O_l under state q_l, and "all Q" here considers all possible underlying state sequences. Equation (3) suggests the full parameter set of a HMM: $\lambda = (\pi, A, B)$, where $\pi = \{\pi_{S_i}\}$ (probability of initial state to be S_i), $A = \{a_{S_i S_j}\}$ (transition probability from state S_i to S_j) and $B = \{b_{S_i}(O)\}$ (probability of observance to be O under state S_i), with $i = \{1, \ldots, N\}$ and $j = \{1, \ldots, N\}$. Since the direct computation of $P(\mathbf{O}|\lambda)$ from Equation (3) is very intensive (requires $2L \times N^L$ operations), an efficient "forward-backward" procedure[20] is carried out by defining two additional variables: the forward variable $\alpha_l(i) = P(O_0 O_1 \ldots O_l, q_l = S_i|\lambda)$ and the backward variable $\beta_l(i) = P(O_{l+1} O_{l+2} \ldots O_{L-1}|q_l = S_i, \lambda)$. In this way the computational complexity of $P(\mathbf{O}|\lambda)$ is reduced to $N^2 L$, a huge save from the computational point of view.

During the *reestimation* (HMM training) procedure, we try to find the model λ of discrete or continuous HMM that leads to a (locally) maximized $P(\mathbf{O}|\lambda)$ for any given training data set. A maximum-likelihood estimation process is realized through an expectation-maximization iterative reestimation procedure[20, 24] in which a previously estimated λ is iteratively replaced by a new estimate $\widehat{\lambda}$ that is provably better than or at least as good as the previous one. The reestimation is repeated to improve the probability until some limit point is achieved. Multiple observation sequences can be used to obtain a reliable estimate of the model parameters. Note that, in practice, since the manipulation of a large number of products involves extremely small probabilities which can exceed the dynamic range of a computer's precision, a scaling procedure is usually applied to the algorithm to ensure that the implementation is numerically stable in finite-precision arithmetic.

In the HMM based damage classifier, features from each structural condition (damage class) are modeled with a separate HMM because the associated physics of the wave propagation is different in each class. In this paper we utilized two types of HMM: the discrete HMM models quantized MPD features, while the continuous HMM models the MPD features directly (without any quantization). Since there is no quantization needed for the continuous HMM, no quantization errors are introduced and more accurate classification results can be expected. However, when dealing with continuous features directly, the computational complexity can be more intensive.

The three major steps for the damage classification are described as follows. First, the time-frequency-scale features are extracted from experimental damage data using L MPD iterations, and an observation sequence $\mathbf{O} = \{O_0, \ldots, O_{L-1}\}$ (composed of the 4-D MPD feature vectors) is obtained for each experimentally measured signal. Second, if discrete HMMs are used, a vector quantization (VQ) procedure is implemented to map each observation O to a discrete symbol from a codebook $V = \{v_1, \ldots, v_K\}$, where K is the size of the codebook. The larger the number of codes K, the smaller is the quantization error. Last, we construct and validate the discrete and continuous HMMs based on experimentally collected data; with the HMMs built, an unknown signal $\mathbf{O}^{\text{test}}$ can be classified to a damage class i according to

$$i = \arg\max_j \log p(\mathbf{O}^{\text{test}}|\lambda_j) \tag{4}$$

with λ_j the trained HMM for jth class. For more details of the proposed HMM based damage classification scheme, the reader is referred to previously published papers.[21, 22]

3. SENSOR FUSION

In the structural damage detection and classification problem, data is usually collected by many distributed sensing devices to exploit the added information from multiple sensors. In such situations, it is desirable to use the data available from all the sensors to produce more accurate and robust performance than what is achievable with only a single sensor. In this paper, we consider two different methods for sensor fusion implementation. The first method is realized based on Bayesian decision fusion where local decisions are first made at each individual sensor and these are then integrated at a decision fusion center to obtain the overall classification.[25] The second method incorporates optimal Bayesian data fusion by directly combining information from the multiple distributed sensors. This depends on the characteristics of the features extracted from the signals: forming a global sequence of feature vectors by combining the locally obtained features vectors.

Let R denote the number of distributed sensors and i the ith damage class. For a given excitation, we define $x^r(t)$ as the response waveform measured by the rth sensor ($r = 1, \ldots, R$), and $\mathbf{O}^r = \{O_0^r, \ldots, O_{L-1}^r\}$ with length L is the corresponding observation sequence of MPD coefficients. With this notation, we now discuss these methods in more detail and outline their advantages and disadvantages.

3.1 Method 1

We employ a Bayesian decision fusion procedure by first performing independent classification using the data collected at each sensor and then integrating these decisions at a fusion center to achieve a global decision. Specifically, in the first step, each signal $x^r(t)$ is assigned to decision u^r based on the HMM classifier discussed

in Section 2, with $u^r = i$ when $x^r(t)$ is assigned to damage class i. Combining the R decisions, we have an assignment vector $\mathbf{u} = \{u^1, \ldots, u^R\}$ and the fusion center declares damage class i based on the rule:

$$i = \underset{j}{\operatorname{argmax}}\, P(\mathbf{u}|j), \tag{5}$$

where $P(\mathbf{u}|j)$ is the probability distribution of the class assignment vector $\mathbf{u}$ given that the damage class is j. Note that the probabilities $P(\mathbf{u}|j)$ are estimated from available training or validation data. Under the assumption of statistical independence of the distributed sensors, $P(\mathbf{u}|j)$ can be factored as

$$P(\mathbf{u}|j) = \prod_{r=1}^{R} P(u^r|j). \tag{6}$$

Inserting this into (5), the global sensor fusion decision becomes

$$i = \underset{j}{\operatorname{argmax}} \prod_{r=1}^{R} P(u^r|j). \tag{7}$$

A block diagram of this sensor fusion algorithm is shown in Figure 1.

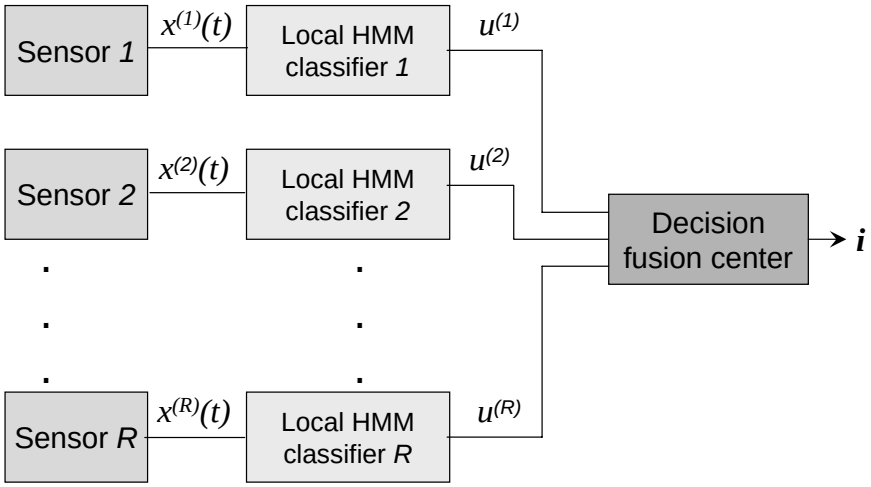

Figure 1. Block diagram of the sensor fusion algorithm using method 1.

3.2 Method 2

The Bayesian decision fusion approach discussed above can lead to significant improvement in the performance of the classifier. However, computational overhead of such a fusion procedure is quite intensive, since it requires training, validating and testing of the individual HMM classifiers to be performed at each sensor. With this complexity, broad use of this approach is impeded, especially for the online damage monitoring in real applications. We therefore consider the optimal Bayesian data fusion technique which is based on the direct joint modeling of the data from all the sensors. This approach integrates information from all the sensors from the beginning by forming fused observation sequences. Training is essentially carried out only once (globally), and the computational complexity is thus drastically reduced. As we observe later, this fusion method also leads to significant improvement in the results as compared to what is achievable with only a single sensor.

Recall that an observation sequence $\mathbf{O} = \{O_0, \ldots, O_{L-1}\}$ is a sequence of L feature vectors, with each vector O composed of the four MPD coefficients $\{\alpha, \kappa, \nu, \tau\}$, thus the dimensionality of this sequence is $L \times 4$. Method 2 for sensor fusion works by first concatenating the sequences of feature vectors $\mathbf{O}^r$, $r = 1, \ldots, R$ from all the sensors to produce a fused sequence of increased dimensionality $(L \times R) \times 4$. The $(L \times 4)$ vectors of the sequence

are then rearranged in ascending order of the corresponding time-shift coefficients (τ). For the MPD time-frequency representation plane, the concatenation and rearrangement of feature vectors equals a superposition of the time-frequency atoms of all the waveforms $\mathbf{O}^r$, $r = 1, \ldots, R$. In this way, the resultant fused "virtual" waveform incorporates information from all the distributed sensors. After obtaining the fused waveforms from different damage classes, the same exact HMM classification algorithm steps (as discussed before in Section 2) are performed. The only difference here is that the data begin modeled now are the fused waveforms of increased dimensionality. In this sense, the resulting final classification is automatically global. The block diagram of this sensor fusion algorithm is shown in Figure 2.

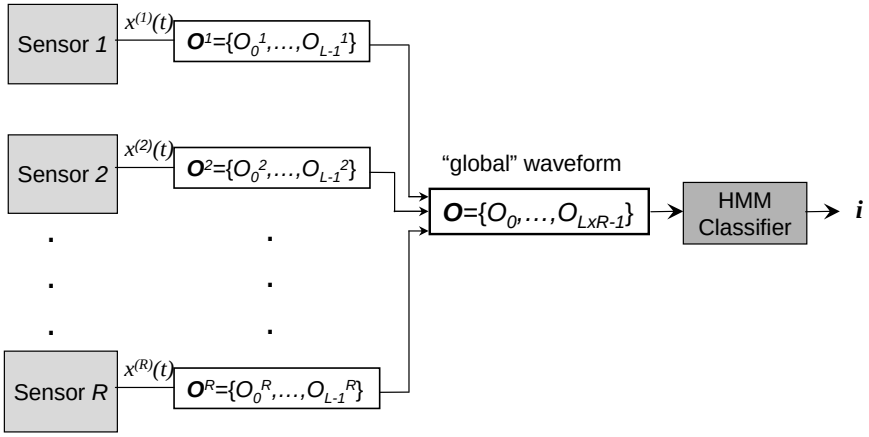

Figure 2. Block diagram of the sensor fusion algorithm using method 2.

We can see that this method of sensor fusion is very easy to implement, since it only requires implementation of the HMM classifier once. It will be observed later in the application section that this method can also yield very good classification performance. One disadvantage of this approach is that due to the increase in the dimensionality of the observation sequences, the quantization codes V (for the discrete HMM) and Gaussian mixtures M (for the continuous HMM) need also to be increased, which in turn increases the required computational effort. However, Method 2 is still less computationally intensive than Method 1, especially when the computational burden is a big concern.

4. APPLICATION TO THE CLASSIFICATION OF DELAMINATION IN A COMPOSITE STRUCTURE

The damage type considered in this paper is the occurrence of delamination in laminated composites. Delamination results from interlaminar stresses that cause joined lamina to develop a discontinuity between them. This makes the laminate both weaker and more compliant. Such interlaminar failures of composite laminates can lead to a reduced ability to support loading. Inability to detect delamination in composite structures, effectively and accurately, is a limiting factor to their use in practice. In this section, we present an application of the proposed HMM damage classifier and the sensor fusion methods to a laminated composite structure for the classification of delamination at different locations.

4.1 Experiment and Data Description

Seeded delaminations at different locations are considered in the laminates. The laminate without delamination is considered as the healthy class. The damage classes are defined as follows: Class 2 signals have a 5% delamination at the 1st interface; Class 3 to Class 7 have 5% delamination at the 2nd to 6th interface. Class 8 signals have a corner delamination at the 4th interface, and Class 9 signals have an edge delamination at the 4th interface. Data is recorded using piezoelectric transducers (PZT) mounted on the structure as shown in Figure 3. A burst signal with a center frequency of 8 kHz is used as the excitation from the center actuator, and the responses are measured at the four PZTs located at the corners. The data sampling frequency is 500 kHz. For each class, we have 360 waveforms to be used for classification.

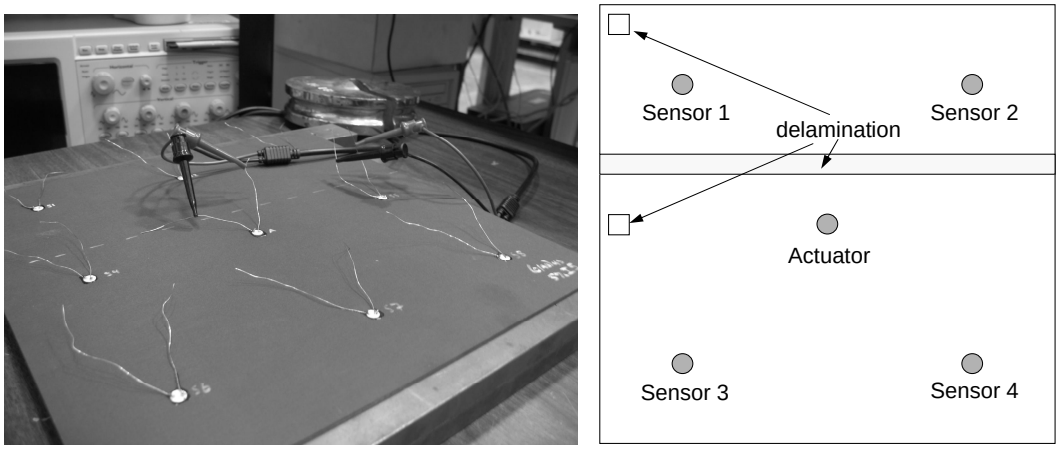

(a) Experiment setup (b) Schematic

Figure 3. Experimental setup for delamination damage in a 292.1 mm× 292.1 mm laminated composite with 5% delamination, and schematic showing the delamination and sensor layout.

As discussed in Section 2, the MPD is first performed on all available waveforms, yielding the corresponding $L \times 4$ observation sequences (here $L = 10$). The time-frequency characteristics of the decomposed waveforms to be modeled by HMMs are explored using the MPD time-frequency representation,[23] which is formed by a linear combination of the Wigner distribution TFRs of each selected Gaussian atom, and Figure 4 shows some example plots of the MPD-TFRs of the waveforms recorded by PZT 3. It can be clearly seen that unique characteristic features are extracted out for each damage; these features can be modeled effectively using the HMMs. These TFRs also serve as a reference for choosing the initial values for the HMM parameters during training. Qualitatively, we see that the time-frequency structures of the signals from different classes generally look different, except for Class 2 and Class 5 signals, and Class 4 and Class 8 signals which are little similar.

4.2 Classification and Results using Individual Classifiers and Sensor Fusion

The available data is divided into three sets: one is for training the HMMs (training set), one for verifying the choice of model parameters (validation set), and the other for testing the individual and global classifier performance (testing set). The purpose of the validation step is to verify the choice of model complexity (the number of states N and the number of Gaussian components M) and parameter initialization. This is a very important step because a bad choice for N and M can lead to HMMs that do not generalize well to a data set from the same class but different from the training set. This problem is solved by verifying the classification performance of the trained HMMs on the experimental validation set, and adjusting the parameter choices if necessary. The resulting HMMs are then used to classify the testing data. Results are presented demonstrating damage classification in the composite examples described above using both discrete and continuous HMMs.

In this paper, the number of HMM states N is estimated by empirical examination of the number of stationarity regions in the MPD-TFRs of the training data. In all the results reported here, N is usually chosen to be around 2 or 3 depending on the damage class in question. Our simulations indicate that the performance of the classifier is not very sensitive to this choice. The associated initial values of the parameters $\lambda = \{A, B, \pi\}$ is also estimated from the TFRs by examining the feature atoms within each defined state. The current empirical estimation of model parameters can be improved by utilizing a variational Bayesian (VB)[22] approach which is designed for automatic estimation of model complexity from the data. The number of HMM training iterations used for training the HMMs is determined based on the convergence of the log-likelihood, which increases monotonically with the training iterations.

The trained HMMs are incorporated into a Bayesian framework for damage classification as discussed in Section 2. Figure 5 shows example plots of the log-likelihood of all the testing data (from PZT 3 for delamination damage) computed by the learnt discrete and continuous HMMs of different classes. The horizontal axis denotes the test signals ordered from Class 1 to Class 9 with 105 waveforms for each class (the vertical lines depict class

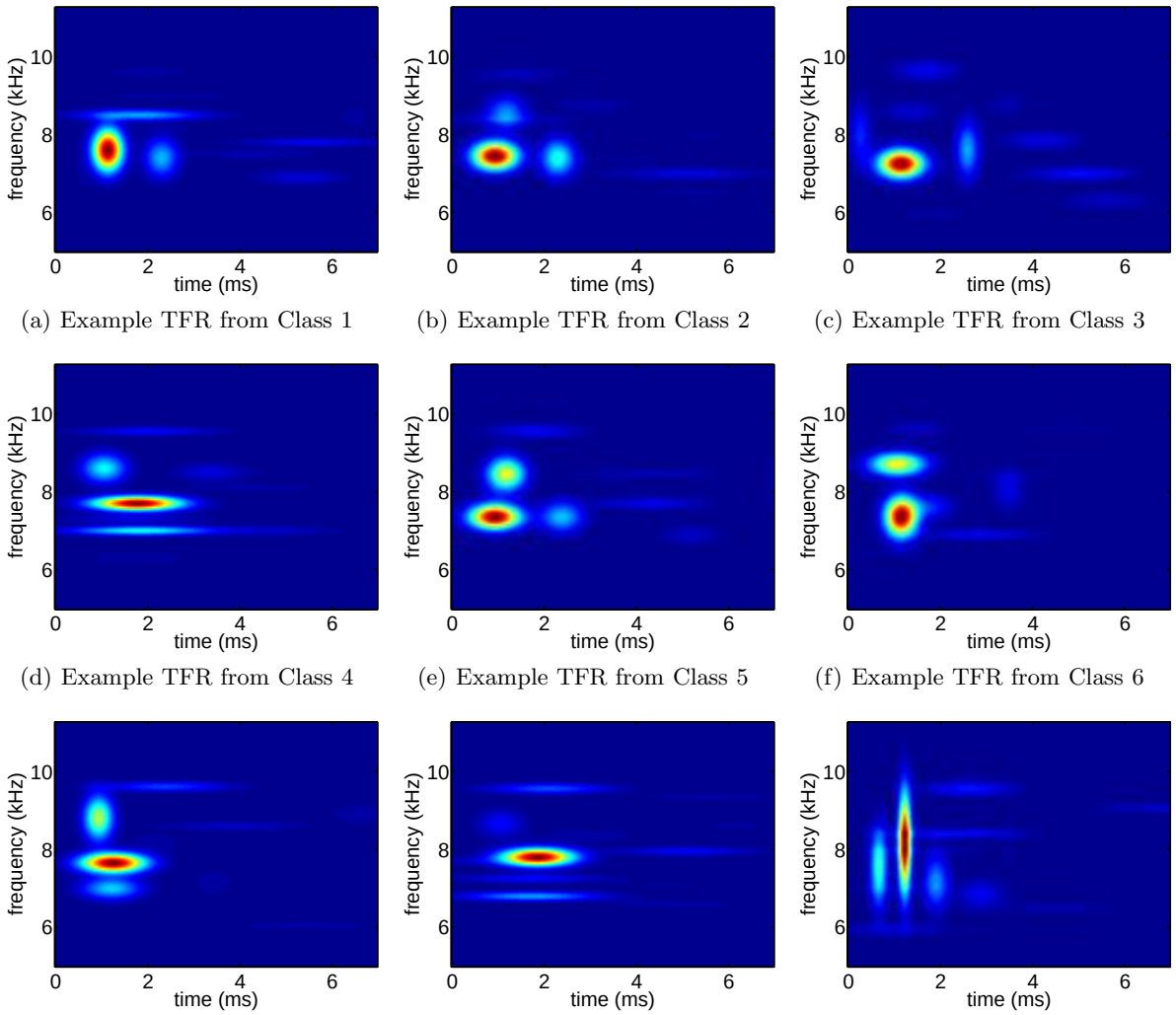

(a) Example TFR from Class 1 (b) Example TFR from Class 2 (c) Example TFR from Class 3

(d) Example TFR from Class 4 (e) Example TFR from Class 5 (f) Example TFR from Class 6

(g) Example TFR from Class 7 (h) Example TFR from Class 8 (i) Example TFR from Class 9

Figure 4. Example TFR plots from all 9 damage classes using recorded waveforms from PZT 3

boundaries). For each signal, nine log-likelihood values computed by the nine HMMs (one for each class) are plotted along the vertical axis. It can be seen that the data from each class generally has the highest likelihood given the HMM trained on that class. The larger the difference in the likelihood from the corresponding HMM and the HMMs associated with the other classes, the more likely it is that the data is classified correctly. From Figure 5, we see that the class separation is greater with the continuous HMM, indicating that more accurate classification can be achieved.

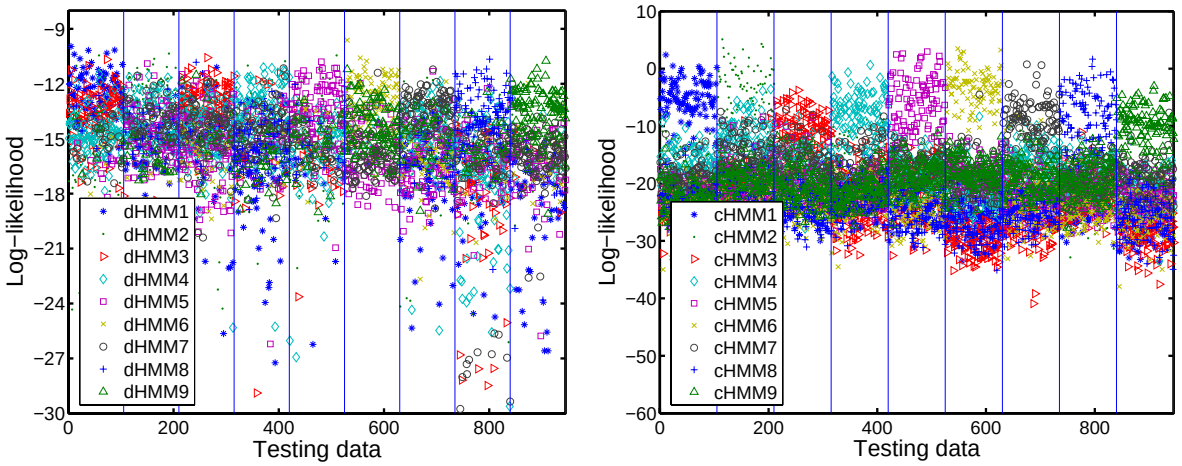

(a) Discrete HMM (b) Continuous HMM

Figure 5. Log-likelihood of the testing data computed by the trained HMMs with "dHMM" denoting "discrete HMM" and "cHMM" denoting "continuous HMM".

4.2.1 Delamination Damage Classification Results

Time-frequency damage features are extracted from each waveform using $L = 10$ iterations of MPD with a dictionary composed of about 1.7 million normalized Gaussian atoms. We stopped the MPD after 10 iterations as that corresponds to a residual signal energy of about 20%. Of the 360 waveforms available for each damage class, 150 waveforms are used for training, 105 are used for validation, and the remaining 105 are used for testing. Using the discrete HMM, the features are quantized using $K = 64$ symbols. Using the continuous HMMs, about $M = 9$ components are used with the Gaussian mixture models. Tables 1 and 2 show the confusion matrices for delamination damage classification using discrete and continuous HMMs, respectively, when only the data from PZT 3 are utilized. We obtain an average correct classification rate of 0.8032 from the discrete HMM and 0.9577 from the continuous HMM. The parameter ξ is an indicator of the classification performance, defined as the mean of the diagonal values of the confusion matrix. The continuous HMM is seen to perform significantly better than the discrete HMM.

Tables 3, 4, 5, and 6 show the confusion matrices for delamination damage classification with the implementation of the two sensor fusion methods discussed in Section 3 both for discrete and continuous HMM classification methods. Compared with the results in Tables 1 and 2, we find that the sensor fusion procedure greatly increases the performance of the classifier (the average correct classification rate ξ is much higher). The correct classification ξ obtained by Method 1 and Method 2 using continuous HMM are 0.9608% and 0.9778%, respectively. Note that in Method 1, the quantity $P(u^r|C_j)$ in Equation (7) (the probability of a waveform from class j being assigned to class $i = u^r$ at sensor r) is simply the element C^r_{ji} of the confusion matrix C^r computed using the validation data from sensor r.

Table 7 summarizes the effect of different choices of model parameters and different sensor fusion implementations on the performance of the proposed classifier for delamination classification. The achieved correct classification rates ξ are tabulated for the discrete HMM (as a function of the number of symbols K) and continuous HMMs, both with and without sensor fusion. As K increases, we see that the performance of the discrete HMM classifier improves and approaches that of the continuous HMM classifier. This is expected, because the quantization error decreases with increasing K.

	class 1	class 2	class 3	class 4	class 5	class 6	class 7	class 8	class 9
class 1	**0.8476**	0.0095	0	0	0.0095	0.0572	0.0571	0.0191	0
class 2	0	**0.7810**	0.0571	0.0381	0.0762	0.0095	0.0286	0	0.0095
class 3	0	0.0762	**0.8762**	0.0095	0	0	0	0	0.0381
class 4	0	0.0095	0.0381	**0.7905**	0.0095	0.0095	0.0857	0.0191	0.0381
class 5	0.0476	0.0762	0	0	**0.6381**	0.0667	0.1143	0.0476	0.0095
class 6	0.0571	0.0857	0.0095	0.0476	0.0191	**0.7524**	0.0191	0.0095	0
class 7	0	0.0667	0	0.0286	0.1523	0.0286	**0.7143**	0	0.0095
class 8	0	0.0191	0	0	0.0667	0.0095	0.0190	**0.8762**	0.0095
class 9	0	0.0667	0.0476	0	0.0095	0	0.0095	0.0191	**0.8476**

Table 1. Confusion matrix for delamination damage classification using discrete HMMs, when only data from PZT 3 is utilized.

	class 1	class 2	class 3	class 4	class 5	class 6	class 7	class 8	class 9
class 1	**0.9810**	0	0	0	0.0095	0	0.0095	0	0
class 2	0	**0.9143**	0.0667	0	0.0095	0	0	0	0.0095
class 3	0	0.0381	**0.9524**	0	0.0095	0	0	0	0
class 4	0	0	0	**1.0000**	0	0	0	0	0
class 5	0	0	0	0	**0.9524**	0.0190	0.0286	0	0
class 6	0	0.0381	0	0	0.0286	**0.9333**	0	0	0
class 7	0	0.0095	0	0	0.0572	0	**0.9333**	0	0
class 8	0	0	0	0	0.0095	0	0	**0.9905**	0
class 9	0	0.0381	0	0	0	0	0	0	**0.9619**

Table 2. Confusion matrix for delamination damage classification using continuous HMMs, when only data from PZT 3 is utilized.

With the sensor fusion implemented, a significant improvement in overall classification performance can be observed. Even when the results from the individual sensors are poor, the improvement using fusion is remarkable. The most accurate classification is shown to be achieved when the continuous HMM and sensor fusion are both utilized. It can also be seen that when discrete HMMs are used, Method 1 yields more accurate classification than Method 2 with the same quantization level. This is attributed to the dimensionality increase of the observation sequences for Method 2, which requires a larger number of levels in the quantization to accurately represent the sequences. When continuous HMMs are used, Method 2 yields performance results comparable to Method 1, while affording lower computational effort since it does not necessitate classifications to be performed locally at each sensor.

	class 1	class 2	class 3	class 4	class 5	class 6	class 7	class 8	class 9
class 1	**0.9810**	0	0	0	0	0.0095	0.0095	0	0
class 2	0.0095	**0.8571**	0.0476	0	0.0286	0.0286	0	0	0.0286
class 3	0	0	**0.9714**	0	0	0.0095	0	0	0.0191
class 4	0	0	0	**0.9238**	0.0191	0.0095	0	0.0095	0.0381
class 5	0.0191	0.0095	0	0.0476	**0.7714**	0.0095	0.1143	0.0286	0
class 6	0.0095	0.0191	0	0.0095	0.0191	**0.9333**	0	0.0095	0
class 7	0	0.0191	0	0	0.1333	0.0095	**0.8286**	0	0.0095
class 8	0	0.0095	0	0	0.0095	0	0	**0.9524**	0.0286
class 9	0.0095	0.0095	0.0191	0	0	0	0.0095	0.0191	**0.9333**

Table 3. Confusion matrix for delamination damage classification using discrete HMMs with the incorporation of sensor fusion using method 1.

	class 1	class 2	class 3	class 4	class 5	class 6	class 7	class 8	class 9
class 1	**1.0000**	0	0	0	0	0	0	0	0
class 2	0.0095	**0.9714**	0	0.0191	0	0	0	0	0
class 3	0.0286	0	**0.9714**	0	0	0	0	0	0
class 4	0.0286	0.0190	0	**0.9524**	0	0	0	0	0
class 5	0.0381	0.0286	0	0.0476	**0.8667**	0	0.0190	0	0
class 6	0.0286	0	0	0	0	**0.9714**	0	0	0
class 7	0.0286	0	0	0	0	0	**0.9714**	0	0
class 8	0.0190	0	0	0	0	0	0	**0.9810**	0
class 9	0.0381	0	0	0	0	0	0	0	**0.9619**

Table 4. Confusion matrix for delamination damage classification using continuous HMMs with the incorporation of sensor fusion using method 1.

	class 1	class 2	class 3	class 4	class 5	class 6	class 7	class 8	class 9
class 1	**0.8857**	0.0190	0	0.0286	0	0.0286	0	0.0381	0
class 2	0.0095	**0.8381**	0	0.1048	0.0286	0	0	0.0095	0.0095
class 3	0.0095	0	**0.7714**	0.0095	0.1619	0.0286	0.0190	0	0
class 4	0.0190	0.0762	0.0190	**0.7714**	0.0762	0.0190	0.0095	0.0286	0
class 5	0.0095	0.0667	0.0762	0.0381	**0.7524**	0.0095	0.0381	0.0095	0
class 6	0.0190	0.0190	0.0571	0.0095	0.0095	**0.8381**	0.0190	0.0286	0
class 7	0.0095	0.1333	0.0190	0.0095	0.0286	0.0381	**0.7333**	0.0095	0.0190
class 8	0.0095	0.0286	0.0095	0	0.0095	0.0571	0	**0.8762**	0.0095
class 9	0	0.0286	0	0	0.0095	0.0286	0.0095	0.0476	**0.8762**

Table 5. Confusion matrix for delamination damage classification using discrete HMMs with the incorporation of sensor fusion using method 2.

	class 1	class 2	class 3	class 4	class 5	class 6	class 7	class 8	class 9
class 1	**1.0000**	0	0	0	0	0	0	0	0
class 2	0	**1.0000**	0	0	0	0	0	0	0
class 3	0	0.0095	**0.9714**	0	0.0095	0	0	0	0.0095
class 4	0	0.0381	0	**0.9048**	0.0571	0	0	0	0
class 5	0	0	0	0	**0.9905**	0.0095	0	0	0
class 6	0	0	0	0	0	**0.9810**	0.0190	0	0
class 7	0	0.0190	0.0095	0	0	0	**0.9524**	0	0.0190
class 8	0	0	0	0	0	0	0	**1.0000**	0
class 9	0	0	0	0	0	0	0	0	**1.0000**

Table 6. Confusion matrix for delamination damage classification using continuous HMMs with the incorporation of sensor fusion using method 2.

	PZT 1	PZT 2	PZT 3	PZT 4	Fusion method 1	Fusion method 2
$K = 64$ (discrete HMM)	0.6603	0.5841	0.7915	0.7037	0.9058	0.7757
$K = 128$ (discrete HMM)	0.7185	0.7016	0.8032	0.7280	0.9122	0.8159
continuous HMM	0.9153	0.9153	0.9577	0.9259	0.9608	0.9778

Table 7. Average correct classification rates ξ for delamination damage classification using discrete and continuous HMMs, with and without sensor fusion.

5. CONCLUSION

In this paper, we presented a damage classification method using the hidden Markov model which statistically models the time-frequency characteristics of experimental damage data. In addition, two methods are proposed to implement sensor fusion. The first method is implemented via a Bayesian decision fusion framework where local decisions are first made at each sensor and are then combined at a decision fusion center to obtain the overall classification. The second method incorporates optimal Bayesian data fusion by directly combining information from the multiple distributed sensors. The proposed classifier and fusion methods are used to classify delamination in a laminated composite. Results show that both methods can produce accurate classification, but the second method is more preferable as it is less computationally intensive than the first method.

We are currently investigating the use of data generated by physically-based finite element (FE) models instead of experimentally collected data to construct the HMMs. Among other things, this is advantageous in situations when enough experimental data is not available for training the classifiers. Experimentally collected signals can then be classified using these model-based HMMs.

ACKNOWLEDGMENTS

This research was supported by the Department of National Aeronautics and Space Administration (NASA) IVHM Grant NNX07AD70A (Program manager: Dr. Steven Arnold).

REFERENCES

[1] Farrar, C. R. and Worden, K., "An introduction to structural health monitoring," *Philosophical Transactions of the Royal Society A* **365**, 303–315 (2007).

[2] Farrar, C. R. and Lieven, N. A. J., "Damage prognosis: the future of structural health monitoring," *Philosophical Transactions of the Royal Society A* **365**, 623–632 (2007).

[3] Baydar, N. and Ball, A., "Case study detectionof gear failures via vibrationand acoustic signals using wavelet transform," *Mechanical Systems and Signal Processing* **17**, 787–804 (2003).

[4] Abdel-Galil, T. K., El-Saadany, E. F., .Youssef, A. M., and Salama, M. M. A., "Disturbance classification using hidden Markov models and vector quantization," *IEEE Transactions on Power Delivery* **20**, 2129–2135 (2005).

[5] Crouse, M. S., Nowak, R. D., and Baraniuk, R. G., "Wavelet-based statistical signal processing using hidden Markov models," *IEEE Transactions on Signal Processing* **46**, 886–906 (1998).

[6] Jeong, H. and Jang, Y., "Fracture source location in thin plates using the wavelet transform of dispersive waves," *IEEE Transactions on Ultrasonics, Ferroelectrics, and Frequency Control* **47**, 612–619 (2000).

[7] Ebenezer, S. P., Papandreou-Suppappola, A., and Suppappola, S. B., "Classification of acoustic emissions using modified matching pursuit," *Journal on Applied Signal Processing* **3**, 347–357 (2004).

[8] Chakrabarti, D., Kovvali, N., Papandreou-Suppappola, A., and Cochran, D., "On the use of matching pursuit decomposition for structural health monitoring," *Journal of Intelligent Material Systems and Structures, special issue on Structural Health Monitoring, under revision* (2007).

[9] Kovvali, N., Das, S., Chakraborty, D., Cochran, D., Papandreou-Suppapola, A., and Chattopadhyay, A., "Time-frequency based classification of structural damage," *48th AIAA/ASME/ASCE/AHS/ASC Structures, Structural Dynamics, and Materials Conference 23 - 26 April 2007, Honolulu, Hawaii, AIAA 2007-2055* .

[10] Sohn, H. and Farrar, C. R., "A statistical process control and projection techniques for structural health monitoring," *European COST F3 Conference on System Identification and Structural Health Monitoring, Madrid, Spain, June 6-9, 2000* .

[11] Sohn, H., Farrar, C. R., Hunter, N. F., and Worden, K., "Structural health monitoring using statistical pattern recognition techniques," *Transactions of the ASME* **123**, 706–711 (2001).

[12] Beck, J. L., Au, S. K., and Vanik, M. W., "A Bayesian probabilistic approach to structural health monitoring," *Proceedings of the American Control Conference San Diego, California June 1999* .

[13] Sohn, H. and Law, K. H., "Application of load-dependent Ritz vectors to Bayesian probabilistic damage detection," *Probabilistic Engineering Mechanics* **15**, 139–153 (2000).

[14] Lee, J. W., Kirikera, G. R., Kang, I., Schulz, M. J., and Shanov, V. N., "Structural health monitoring using continuous sensors and neural network analysis," *Smart Mater. Struct.* **15**, 1266–1274 (2006).

[15] Kim, S. D., In, C. W., Cronin, K. E., Sohn, H., and Harries, K., "Application of outlier analysis for baseline-free damage diagnosis," *Proc. of SPIE* **6174**, 6174H (2006).

[16] Park, G., Rutherford, A. C., Sohn, H., and Farrar, C. R., "An outlier analysis framework for impedance-based structural health monitoring," *Journal of Sound and Vibration* **286**, 229–250 (2005).

[17] Sohn, H., Allen, D. W., Worden, K., and Farrar, C. R., "Structural damage classification using extreme value statistics," *Journal of Dynamic Systems, Measurement, and Control* **127**, 125–132 (2005).

[18] Das, S., Srivastava, A. N., and Chattopadhyay, A., "Classification of damage signatures in composite plates using one-class SVMs," *Aerospace Conference, 2007 IEEE 3-10 March 2007* , 1–19.

[19] Rabiner, L. R. and Juang, B. H., "An introduction to hidden Markov models," *IEEE ASSP Magazine* , 4–15 (1986).

[20] Rabiner, L. R., "A tutorial on hidden Markov models and selected applications in speech recognition," *Proceedings of the IEEE* **77**, 257–286 (1989).

[21] Zhou, W., Kovvali, N., Papandreou-Suppappola, A., Cochran, D., and Chattopadhyay, A., "Hidden Markov model based classification of structural damage," *Proc. of SPIE* **6523**, 652311 (2007).

[22] Zhou, W., Chakraborty, D., Kovvali, N., Papandreou-Suppappola, A., Cochran, D., and Chattopadhyay, A., "Damage classification for structural health monitoring using time-frequency feature extraction and continuous hidden Markov models," *Asilomar Conference on Signals, Systems, and Computers* (2007).

[23] Mallat, S. G. and Zhang, Z., "Matching pursuits with time-frequency dictionaries," *IEEE Transactions on Signal Processing* **41**, 3397–3415 (1993).

[24] Bilmes, J. A., "A gentle tutorial of the em algorithm and its application to parameter estimation for gaussian mixture and hidden Markov models," *International Computer Science Institute* , 1–13 (1998).

[25] Zhou, W., Kovvali, N., Papandreou-Suppappola, A., Cochran, D., Reynolds, W., and Chattopadhyay, A., "Classification of damage in composite structures using hidden Markov models for integrated vehicle health management," *Journal of Intelligent Material Systems and Structures, special issue on Structural Health Monitoring, under revision* (2007).